



VISUALIZING LIGHT CONES IN SCHWARZSCHILD SPACE

TARIG ELMABROUK AND ROBERT J. LOW

Communicated by Gregory L Naber

Abstract. We present a numerical approach to the visualization of the light cones, and hence the causal structure, of exterior Schwarzschild space, taking advantage of the symmetries of Schwarzschild space and the conformal invariance of null geodesics.

1. Introduction

The purpose of this paper is to describe a numerical tool for the investigation of the causal structure of exterior Schwarzschild space by visualization of the light cones. The tool should also be of use to an instructor teaching a course including material on the causal structure of space-time, or to a student on such a course. Much of the material should be accessible to a student of general relativity who has previously studied a course at the level of, for example, d’Inverno [3] or Hughston and Tod [2], and the tool should help to bridge the gap between such texts and the more advanced treatments of Wald [8] or Hawking and Ellis [1]. We will use the Einstein summation convention throughout.

In Section 2, we provide a brief review of the causal structure of Minkowski space, as is generally discussed in introductory courses on special relativity, and how this generalizes to general space-times, with particular reference to the importance of null geodesics. In Section 3, we consider static space-times, and demonstrate how conformal transformations can be used to reduce the problem of finding null geodesics in space-time to that of finding geodesics in a Riemannian manifold of lower dimension. Section 4 carries this procedure out in the case of exterior Schwarzschild space-time. In Section 5 we provide a description of the numerical approach used, with some illustrative figures. Section 6 briefly discusses how the visualization tool might be used as an educational tool. The code itself is freely available to download.

2. Causal Structure

We begin by reviewing the causal structure of Minkowski space-time, and seeing how these ideas generalise to curved space-time.

So let \mathbb{M} be Minkowski space-time, with the standard coordinates $(x, y, z, t) = (x^1, x^2, x^3, x^4)$, in units in which $c = 1$. We will take x^α as an abbreviation for (x^1, x^2, x^3, x^4) , with α (and Greek indices generally) being understood to take values 1, 2, 3, 4. The inner product on \mathbb{M} is then $\eta = \text{diag}(1, 1, 1, -1)$.

Given two events, P and Q in \mathbb{M} , with coordinates x_P^α and x_Q^α the vector connecting P to Q is $\overrightarrow{PQ} = v^\alpha = x_Q^\alpha - x_P^\alpha$, and a particle travelling with constant velocity from P to Q is travelling slower than light, at the speed of light, or faster than light as $v^\alpha v^\beta \eta_{\alpha\beta}$ is negative, zero, or positive, and we say that v^α is timelike, null, or spacelike respectively. Since the third possibility implies the ability to send a message into one's own past, we exclude it as the possible trajectory of a physical particle.

If $t_Q \geq t_P$, then in the first case a massive particle can travel from P to Q , we say that Q is to the chronological future of P , and we write $Q \in I^+(P)$. In the second case only a massless particle can, and we say that Q is to the causal future of P , and write $Q \in J^+(P)$. I^- and J^- , the chronological and causal past are defined by $Q \in I^-(P)$ if and only if $P \in I^+(Q)$ and $Q \in J^-(P)$ if and only if $P \in J^+(Q)$. Finally, $I(P)$ is defined to be $I^+(P) \cup I^-(P)$ and $J(P)$ is $J^+(P) \cup J^-(P)$.

The light cone of P is the set of all events in \mathbb{M} which are connected to P by a null vector, and it forms the boundary of $I(P)$: the interior of his light cone comprises the chronological future and past of P .

Lucid descriptions of these notions can be found in the standard texts, such as Rindler [6] or Taylor and Wheeler [7], while a detailed consideration of the causal geometry of Minkowski space and some of its less widely appreciated aspects is provided in Naber [5].

These definitions of chronological future and past do not easily generalize, however: an alternative characterization is used.

If $x^\alpha(s)$ is a curve in \mathbb{M} , parametrized by s , then the tangent vector to this curve at each event is given by \dot{x}^α , and the curve is said to be spacelike, timelike, or null at $x^\alpha(s)$ as \dot{x}^α is spacelike, timelike or null: a timelike vector is said to be future pointing if $\dot{x}^4 > 0$, and past pointing if $\dot{x}^4 < 0$.

Then it is fairly obvious, and not too difficult to prove [5], that $Q \in I^+(P)$ if and only if there is a curve which starts at P , ends at Q , and has future pointing timelike tangent vector at each point. The Q lies on the future light cone of P

if and only if there is a curve starting at P and ending at Q whose tangent is everywhere future pointing and null, but $Q \notin I^+(P)$.

This latter is the characterization which we must use in a general space-time. If M is space-time with metric $g_{\alpha\beta}$, then there is a null cone at each point consisting of those tangent vectors n^α such that $g_{\alpha\beta}n^\alpha n^\beta = 0$. At each point, this null cone splits into two halves: if it is possible to choose one of these halves consistently over the whole of M , we say that M is time orientable, and arbitrarily choose one of the halves to be the future half.

We can now consider a curve $x^\alpha(s)$ in M , and its tangent vector \dot{x}^α at each point. We define this curve to be timelike, null or spacelike at $x^\alpha(x)$ depending on the sign of $g_{\alpha\beta}\dot{x}^\alpha\dot{x}^\beta$ just as before: and in the first two cases to be future pointing if the vector points into the future half of the light cone, and past pointing otherwise.

Finally, we say that $P \in I^+(Q)$ if there is a curve from P to Q whose tangent vector is everywhere timelike and future pointing, and $P \in J^+(Q)$ if there is a curve from P to Q which is everywhere timelike or null and future pointing; and similarly for I^- and J^- .

These relationships define the causal structure of a space-time, since they determine the pairs of events P and Q such that a signal can propagate from P to Q : in other words such that the situation at P can influence the situation at Q . This is clearly a fundamental property of space-time. The question then arises, given P , how can we tell just which events comprise $I^+(P)$?

The situation is similar to that of Minkowski space, but not identical. We now call the set of events which are connected to P by a null geodesic, the light cone of P . Note the distinction between the null cone of P , which is the set of null vectors in the tangent space to M at P , and the light cone of P , which is the set of points in M connected to P by a null geodesic. Then one might hope that, as before, the light cone of P forms the boundary of $I^+(P)$. Unfortunately, this is not the case in general. In a general space-time, there may be points on the boundary of $I^+(P)$ which cannot be connected to P by a null geodesic, and points on future pointing null geodesics emanating from P which are inside $I^+(P)$ rather than on the boundary.

Fortunately, we are restricting our attention to Schwarzschild space, in which the first situation is not an issue: null geodesics can be extended to arbitrarily large values of t . The second situation is the one which affects us. This arises when distinct null geodesics emanating from an event P eventually meet and cross: after they have crossed, each has passed through the boundary of $I^+(P)$ to the interior of $I^+(P)$. The boundary of $I^+(P)$ is thus given by the light cone of P , up to the point where null geodesics intersect.

Note that this is telling us something significant: the null geodesics meet because of gravitational focussing, i.e., the presence of a gravitational lense. In other words, although gravitational lensing is generally studied in a first course in general relativity, but causal structure is not, the phenomenon of gravitational lensing is intimately bound up with the presence of non-trivial causal structure.

In the next two sections we will see how the light cones of space-times with the symmetry of exterior Schwarzschild can be described, and produce some sample diagrams obtained from a numerical approach.

3. Static Space-Times

First, we specialize from general space-times to static space-times, i.e. space-times which have a coordinate system (x^a, t) (where $a = 1, 2, 3$, as do Latin indices in general) in which the metric takes the form

$$g_{ab}(x^a)dx^a dx^b - f(x^a)dt^2$$

where $f(x^a) > 0$, so that the metric is independent of time.

Exterior Schwarzschild is, of course, of this form, but before considering that particular case we will see how the symmetry of time-invariance simplifies the problem of finding the null geodesics.

It is immediately obvious that if we make a conformal transformation, i.e., replace the metric $g_{\alpha\beta}$ by the metric $\tilde{g}_{\alpha\beta} = e^{\Omega}g_{\alpha\beta}$ where Ω is any smooth function on space-time, then the causal classification of vectors, and hence curves, is unchanged. It follows that the metrics $g_{\alpha\beta}$ and $\tilde{g}_{\alpha\beta}$ determine the same causal structure. Less obviously, the two metrics have the same null geodesics, and this is what we will take advantage of.

For in a general space-time, M , with metric $g_{\alpha\beta}$, and affinely parameterised geodesic is a curve $x^\alpha(s)$ satisfying the differential equation

$$\ddot{x}^\alpha + \Gamma_{\beta\gamma}^\alpha \dot{x}^\beta \dot{x}^\gamma = 0$$

where the $\Gamma_{\beta\gamma}^\alpha$ are the usual Christoffel symbols.

Now, if we consider the metric $\tilde{g}_{\alpha\beta}$, and denote by F_α the partial derivative of F with respect to x^α for any smooth function F , then

$$\tilde{\gamma}_{\beta\gamma}^\alpha = \frac{1}{2}\tilde{g}^{\alpha\delta}(\tilde{g}_{\gamma\delta,\beta} + \tilde{g}_{\beta\delta,\gamma} - \tilde{g}_{\beta\gamma,\delta}) = \Gamma_{\beta\gamma}^\alpha + \frac{1}{2}g^{\alpha\delta}(\Omega_{,\beta}g_{\gamma\delta} + \Omega_{,\gamma}g_{\beta\delta} - \Omega_{,\delta}g_{\beta\gamma}).$$

It then follows that if

$$\ddot{x}^\alpha + \Gamma_{\beta\gamma}^\alpha \dot{x}^\beta \dot{x}^\gamma = 0$$

then

$$\ddot{x}^\alpha \tilde{\Gamma}_{\beta\gamma}^\alpha \dot{x}^\beta \dot{x}^\gamma = \ddot{x}^\alpha \Gamma_{\beta\gamma}^\alpha \dot{x}^\beta \dot{x}^\gamma + \dot{\Omega} \dot{x}^\alpha + \frac{1}{2} g^{\alpha\delta} \Omega_{,\delta} \dot{x}^\beta \dot{x}^\gamma$$

where $\dot{\Omega}$ is the derivative of Ω along the curve $x^\alpha(s)$.

But in the case where \dot{x}^α is everywhere null, this reduces to

$$\ddot{x}^\alpha + \tilde{\Gamma}_{\beta\gamma}^\alpha \dot{x}^\beta \dot{x}^\gamma = \dot{\Omega} \dot{x}^\alpha$$

which is differential equation for a geodesic not parametrized by an affine parameter.

So null geodesics are preserved, although the affine parametrization is not. This might at first sight seem like a problem, but we will see below that in fact it is an advantage.

Let us now return to the problem of describing the null geodesics in a static space-time. We have the metric

$$g_{ab} dx^a dx^b - f(x^a) dt^2$$

and we now know that the null geodesics of this metric are the same as those of the metric

$$\tilde{g}_{ab} dx^a dx^b - dt^2$$

where $\tilde{g}_{ab} = g_{ab}/f(x^a)$, so can find the null geodesics of the original space-time by finding the null geodesics of this one.

But the geodesic equations have now become

$$\ddot{x}^a + \Gamma_{bc}^a \dot{x}^b \dot{x}^c = 0, \quad \ddot{t} = 0$$

where Γ_{bc}^a are the Christoffel symbols of the three dimensional Riemannian metric $\tilde{g}_{ab} = g_{ab}/g(x^a)$.

We immediately see that if $(x^a(t), t)$ is a null geodesic in M parameterized by t (which is not, in general, an affine parameter), then $x^a(t)$ will be an arc-length parameterized geodesic of the Riemannian metric \tilde{g}_{ab} , and vice versa. We can thus construct the null geodesics of M finding the arc-length parameterized geodesics of \tilde{g}_{ab} and associated to each $x^a(t)$ in the Riemannian space, the corresponding $(x^a(t), t)$ in space-time.

The unexpected advantage of this approach is that when we visualize the null cone of an event, P , it will be convenient to compute the section of the null cone between two values of t , the time coordinate. If we were to work with an affine parameter, we would have the additional complication of continuing to evolve each null

geodesic until the affine parameter gave the required value of $t(s)$. This complication does not arise when we are effectively parameterizing the null geodesics by t in the first place.

So far, we have reduced the dimension of the problem by one by using the time symmetry present in Schwarzschild space-time. Next, we take advantage of the spherical symmetry.

4. Schwarzschild Space-Time

We will use the standard polar coordinates for exterior Schwarzschild space-time, in which the metric takes the form

$$\frac{1}{1 - 2M/r} dr^2 + r^2(d\theta^2 + \sin^2\theta d\phi^2) - \left(1 - \frac{2M}{r}\right) dt^2$$

for $r > 2M$, and which we immediately replace by the conformally related metric

$$\frac{dr^2}{\left(1 - \frac{2M}{r}\right)^2} + \frac{r^2}{1 - \frac{2M}{r}}(d\theta^2 + \sin^2\theta d\phi^2) - dt^2 \quad (1)$$

from which in turn we extract the Riemannian metric

$$\frac{dr^2}{\left(1 - \frac{2M}{r}\right)^2} + \frac{r^2}{1 - \frac{2M}{r}}(d\theta^2 + \sin^2\theta d\phi^2). \quad (2)$$

Then a null geodesic of Schwarzschild space-time, parameterized by time, is an affinely parameterized null geodesics of the conformally related metric (1), given by $(r(t), \theta(t), \phi(t), t)$, where $(r(t), \theta(t), \phi(t))$ is a geodesic of the Riemannian metric (2) parameterized by arc-length.

We now make the final simplification, which takes advantage of the spherical symmetry of Schwarzschild space: this relies on the familiar facts (see, for example, Hughston and Tod [2]) that a geodesic which initially lies in and is tangent to the equatorial plane $\theta = \pi/2$ remains in that plane, and that by suitable rotation, any geodesic can be put in this form. We thus obtain our final Riemannian metric

$$\frac{dr^2}{\left(1 - \frac{2M}{r}\right)^2} + \frac{r^2}{1 - \frac{2M}{r}} d\phi^2 \quad (3)$$

with the associated Lagrangian

$$L = \frac{\dot{r}^2}{\left(1 - \frac{2M}{r}\right)^2} + \frac{r^2}{1 - \frac{2M}{r}} \dot{\phi}^2.$$

The equations of the arc-length parameterized geodesics of the final metric (3) are the Euler-Lagrange equations of this Lagrangian, which are easily found to be

$$\ddot{r} = \dot{r}^2 \frac{2M}{r(r-2M)} + \dot{\phi}^2 (r-3M), \quad \ddot{\phi} = 2\dot{\phi}\dot{r} \frac{3M-r}{r(r-2M)}.$$

The solutions of these equations can then be used to construct the null geodesics, and hence the light cones, in the equatorial plane in exterior Schwarzschild space-time: because of the spherical symmetry, a rotation in each surface of constant t about an axis containing the point $r = 0$ and the spatial coordinates of the event P recovers the full light cone of P .

5. Visualizing the Light Cones

Now, the solutions of the geodesic equations cannot be expressed in terms of the standard elementary functions, so instead we solve the equations numerically. For simplicity, we take $M = 1$, so that the event horizon is at $r = 2$ and the photon sphere at $r = 3$. The visualization tool we now describe was developed in MATLAB, which conveniently combines built-in routines for solving differential equations and excellent graphical output which allows the user to interact fruitfully with the figures.

The first routine¹ is `wave_front_s.m`. It provides an interactive means of investigating the development of light cones in the vicinity of a Schwarzschild black hole.

The user is prompted for values of

1. the amount of coordinate time for which the development should be studied
2. the initial radial coordinate of the point (which we give initial time coordinate $t = 0$)
3. the range of initial tangent directions, and
4. the number of geodesics to compute.

This allows the user to investigate how the behaviour depends on distance from the event horizon, to focus on ranges of particular interest, and to choose how finely detailed an image is produced.

As an example, we show the dialogue produced by a choice of 15 for the development time, an initial radial coordinate of 3 (so that the initial point lies on the

¹http://www.bio21.bas.bg/jgsp/m_files/wave_front_s.m

photon sphere), the range $[-\pi, \pi]$ for tangent directions (so the full circle is produced), and 200 for the number of geodesics to be plotted

```

Enter the evolution time period: 15
Enter the initial radial coordinate: 3
Enter the range of tangent directions you
want to investigate in the form [start end]: [-pi pi]
Enter the number of directions: 200

```

The output from MATLAB then conveniently produces the top-down view in Fig. 1, showing the projection of the geodesics to a surface of constant t , where r and ϕ are treated as standard plane polar coordinates.

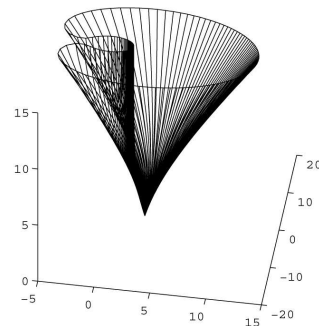
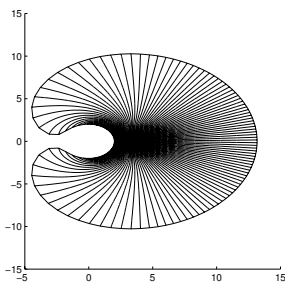


Figure 1. Top Down View of Light Cone. **Figure 2.** Rotated View of Light Cone.

In this figure, the lines emanating from the point P with coordinates $r = 3, \phi = 0$ are the null geodesics, and we can see how they are deflected and spread out by the black hole. Allowing the development to continue for a little longer would let a pair of null geodesics meet. Then an observer at the point at which they meet would see the point of origin at each side of the black hole. Recalling that the full situation is obtained by rotating about an axis connecting the origin of the plane P , we see that this produces the famous Einstein ring. Then, allowing the light cone to develop slightly further, we enter the situation where some of the null geodesics no longer lie on the boundary of $I^+(P)$, but enter $I^+(P)$.

But the user can also now interact with this figure, zooming, panning and rotating at will, to produce other images, such as that of Fig. 2, in which the ‘vertical’ axis is time, and which now shows how the null geodesics (at least initially) form the boundary of $I^+(P)$. We can also see more clearly how the light cone of P develops, in particular how it wraps around the event horizon at $r = 2$ without crossing it.

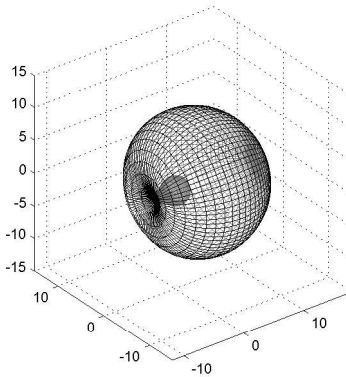


Figure 3. The Light Cone at $t = 15$.

We emphasize that these are only illustrative figures. The real power of this program is to allow the user to investigate different choices of initial conditions and to interact with the graphics in order to gain a better appreciation of how the light cones develop, and so of the causal structure of Schwarzschild space.

This gives a space-time view of the development of light cones in the equatorial plane of exterior Schwarzschild, at the expense of one of the spatial dimensions.

The second program², `wave_front_3d_s.m`, produces an animation of the growth of the full light cone in three spatial dimensions by rotating the equatorial section about the axis of symmetry: in this version, the default is to compute the entire sphere, and the user selects the initial event, the time of development, the number of geodesics to compute in the equatorial plane, and the number of frames to build for the animation.

The dialogue to produce a 20 frame animation of the three-dimensional growth of the light cone considered above is

```
Enter the evolution time period: 15
Enter the initial radial coordinate: 3
Enter the number of geodesics to compute: 150
How many frames? 20
```

An example frame, showing the $t = 15$ section of the light cone of P , is given in Fig. 3. Again we emphasize that it is from interaction with the programs that the user benefits, rather than from viewing these static samples: in this case, he can

²http://www.bio21.bas.bg/jgsp/m_files/wave_front_3d_s.m

observe the development of the light cone as a growing wave-front, and tune the point of view, transparency etc as desired by adjusting the source code.

6. Discussion

The MATLAB programs provide a tool for the user to investigate the development of light cones in Schwarzschild space-time, and so to encourage a better understanding of the causal structure. They can also be used as a teaching tool, helping to illustrate topics such as

1. the relationship between the light cone and the chronological relation
2. how null geodesics are focussed or spread out in Schwarzschild space-time
3. the nature of conjugate points, and how they differ from points where distinct null geodesics through a common initial even subsequently cross.

We intend to develop this to a general purpose tool for investigating the development of light cones in static space-times with two spatial dimensions, taking advantage of MATLAB's symbolic manipulation package to compute the required connection coefficients after the user has specified the metric. The approach is intended to be complementary to that given by Müller and Frauendiener's [4] geodesic visualization tool. Rather than providing high-quality investigations into the growth of individual geodesics in a specific selection of space-times, the software will give the option of a range of quick-and-crude (by choosing a small number of geodesics) or slow-and-detailed (by choosing a large number) interactive investigations of the growth of light cones in a user-specified static space-time.

References

- [1] Hawking S. and Ellis G. *The Large Scale Structure of Space-Time*, Cambridge University Press, London 1973.
- [2] Hughston L. and Tod K., *General Relativity*, Cambridge University Press, Cambridge 1994.
- [3] d'Inverno R., *Introducing Einstein's Relativity*, Clarendon Press, Oxford 1992.
- [4] Müller T. and Frauendiener J., *Studying Null and Timelike Geodesics in the Classroom*, Eur. J. Physics, **32** (2011) 747.
- [5] Naber G., *Geometry of Minkowski Space*, Springer, New York 1992.

-
- [6] Rindler W., *Special Relativity*, Clarendon Press, Oxford 1991.
[7] Taylor E. and Wheeler J., *Spacetime Physics*, Freeman, San Francisco 1992.
[8] Wald R., *General Relativity*, Chicago University Press, Chicago 1984.

Tarig Elmabrouk
Department of Mathematics
and Control Engineering
Coventry University
Priory Street
Coventry CV1 5FB
UK
E-mail address: elmabrot@uni.coventry.ac.uk

Robert J Low
Department of Mathematics
and Control Engineering
Coventry University
Priory Street
Coventry CV1 5FB
UK
E-mail address: mtx014@coventry.ac.uk